8-2020

Application of optimized laser surface re-melting process on selective laser melted 316L stainless steel inclined parts

Jafar Ghorbani
The University of Texas Rio Grande Valley

Jianzhi Li
The University of Texas Rio Grande Valley

Anil K. Srivastava
The University of Texas Rio Grande Valley

Recommended Citation

Ghorbani, Jafar, Jianzhi Li, and Anil K. Srivastava. "Application of optimized laser surface re-melting process on selective laser melted 316L stainless steel inclined parts." Journal of Manufacturing Processes 56 (2020): 726-734. https://doi.org/10.1016/j.jmapro.2020.05.025

Application of Optimized Laser Surface Re-melting Process on Selective Laser Melted 316L Stainless Steel Inclined Parts

Jafar Ghorbani, Jianzhi Li*, Anil K. Srivastava
Department of Manufacturing and Industrial Engineering,
The University of Texas Rio Grande Valley, Edinburg, TX 78539, USA

* Corresponding author.
E-mail address: jianzhi.li@utrgv.edu (J. Li)

Lower surface quality of selective laser melting (SLM) manufactured parts remains to be a key shortcoming particularly for high performance functional components. In this paper, the authors utilized Box-Behnken methodology to explore the effect of laser surface re-melting process parameters. The process parameters are:laser power, laser exposure time, laser point distance, and shell layer thickness. The experiments were conducted using Renishaw AM-250 machine. SLM manufactured parts with inclination of 45˚ up-skin were treated with a given surface roughness using laser surface re-melting (LSR). The optimization of process parameters was conducted using response surface methodology and the validation tests was carried out utilizing the determined input parameters. The results verified the effectiveness of the integrated approach and the proposed statistical model. The outcomes of this study demonstrated that selective laser melting process followed by the laser surface re-melting process is very likely to become a fast and economic integrated method for improving the inclined surface quality of SLM manufactured parts.

Keywords: Additive manufacturing, Laser re-melting, Surface quality, Inclined surface roughness, 316L stainless steel, Design of experiment, Selective laser melting (SLM), Box-Behnken design

1 Introduction

Additive manufacturing technologies have profoundly changed the paradigm of manufacturability and production concepts in both industry and academia, in particular, over last decades. Improving efficiency in particular for low volume productions, allowing higher geometrical flexibility in design, not requiring molds and special tooling are among top advantages of AM technologies [1]. Additive manufacturing (AM), also known as direct digital manufacturing (DDM) or 3D printing, refers to a series of emerging layer-by-layer fabrication from 3D CAD models technologies which in lieu of conventional material removing approach focus on layer by layer material adding approach [2]. The American Society for Testing and Materials (ASTM) categorized widely used AM methods into seven groups including directed energy deposition, sheet lamination, powder bed fusion, material extrusion, binder jetting, material jetting, and VAT photo-polymerization [3].

Selective laser melting (SLM), selective laser sintering (SLS), and electron beam melting (EBM) are three main techniques of powder bed fusion based additive manufacturing (AM) technologies which are widely used for additively manufacturing of near-net-shape metallic, polymeric, ceramic, and composite components [4]. SLM has been increasingly gaining both academia and industry attention due to high performance and low costing comparing to conventional subtractive processes when dealing with small batch size. It is also an increasingly attractive process of choice for fabrication of components with internal features and/or complex geometries in particular for automotive, aerospace, and medical applications [5].

316L stainless steel used in SLM, is among major metallic alloys which have been most extensively studied over last decade due to its superior ductility, weldability, corrosion and oxidation resistance, biocompatibility, relatively low cost, and various applications in different industries including oil and gas, aerospace, chemical plants, and automotive [6]. However, the lower surface quality of SLM manufactured parts has been a problem for industry fore-runners to spread this technology to actual industry productions [7]. Typical average roughness value of components manufactured by conventional mechanical techniques such as grinding and milling is less than 1-2 μm. However, the average roughness value of SLM fabricated parts is typically between 10 and 30 μm [8]. Powder characteristics, process parameters, part complexity, and part location on the substrate affect the surface quality of SLM manufactured components [9]. Inferior surface quality and dimensional inaccuracy necessitate post processing treatment for almost all AM technologies [10]. Recent review by Ernesto et al. [11] revealed that about 40% of studies on surface properties evaluation on AM fabricated parts focused on stainless steel alloys, 35% on titanium alloys, less than 10% on aluminum alloys and remaining on nickel alloys and refractory materials. Within stainless steel alloys, 316L is the most studied alloy for SLM components due to its wide industrial applications.

Post processing treatment and process parameters optimization are two main approaches for improving the surface quality of SLM components [12]. Main processing parameters for SLM include laser power, laser beam diameter, laser point distance, laser speed, laser hatch distance, layer thickness, laser beam focal offset, scanning strategy, inert gas concentration, and so on. Most of the SLM process optimization studies considered laser power, hatch spacing and scanning speed as the vital process inputs for surface roughness improvement [13]. ~~Sand blasting, shot peening, machining, polishing, chemical etching, barrel finishing, laser surface modification and plasma spraying are among the most common mechanical, thermal, or chemical surface modification options. However, these post processing procedures are labor-intensive and relatively slow, and particularly challenging to implement on SLM components which typically have very intricate geometry and internal features. Another challenge in this area is that, the more complex is geometry and internal features, the more difficult is implementation of these post process surface finishing~~ There are numerous mechanical, thermal, or chemical surface modification techniques such as sand blasting, shot peening, machining, polishing, chemical etching, barrel finishing, and plasma spraying which can be implemented as post processing step to improve surface roughness and other properties. However, these post processing tools are labor-intensive and relatively slow, and particularly challenging to implement on parts with very intricate geometry and internal features [14-17]. Baicheng et al. [18] enhanced surface roughness to as low as 3.66 μm (Ra), from the initial surface roughness of 6.05 μm on Inconel 718 SLM manufactured components by applying electrochemical polishing post process including 20% vol. sulphuric acid solution.

Laser surface modification process has a distinguished feature among surface modification tools. Since both selective laser melting and laser surface modification use the same source of energy (i.e. Laser), laser surface re-melting process could be applied either as post surface modification technique or as integrated part of selective laser melting machine [8, 19]. Alfieri et al. [20] applied laser surface modification as a post processing treatment on the surface of UNS S17400 chromium-copper precipitation hardening steel SLM manufactured parts on 45˚ inclined surfaces which was resulted in up to 92% surface roughness improvement (best obtained surface roughness, Ra=1.34 µm). Alrbaey et al. [21] utilized design of experiments methodology and laser surface re-melting (LSR) as a post processing tool to optimize inclined surface roughness of SLM manufactured 316L stainless steel parts. Their findings showed that LSR in post process mode could decrease inclined surface roughness to as low as 1.4 µm ±10%. However, they noticed slight damage to the edges of the components due to the large laser spot size (hatch spacing 400 µm; and beam spot size: 1 mm) which was utilized in thier study. Wang et al. [8] investigated the influence of laser surface re-melting on the top surface roughness of SLM fabricated 316L stainless steel parts (laser power: 150 W, layer thickness: 80 µm, scanning speed: 600mm/s). They were able to decrease SLM manufactured top surface roughness from 14.33 µm to 8.20 µm and from 14.33 to 3.34 µm after two (2) and five (5) times repeating of re-melting process, respectively. They also concluded that more factors play roles for improving the curved or inclined surface roughness rather than top surface roughness. Kruth et al. [22] conducted a comprehensive study in order to improve top surface roughness of 316L SLM manufactured parts by surface laser re-melting process within the same machine. But to find the optimized set of influential process parameters they used single factor experiments and several test series instead of design of experiments systematic approach. They enhanced the top surface quality remarkably (R_a from 15 µm to 1.5 µm) by repeating LSR process five (5) times. Yasa and Kruth [23] used optimized process parameters of laser top surface re-melting which they obtained through single factor experiments and test series for improving the inclined surface roughness. In fact, by laser surface re-melting on 316L SLM fabricated inclined parts (200 mm/s, 95 W, a scan spacing of 60 µm, 10 re-melting scans) they reduced inclined surface roughness from 12 µm to around 3.5 µm on inclined angles of 10˚, 30˚ and 50˚.

To the best of authors' knowledge, current work is the first time that design of experiment tool is applied on laser surface re-melting process parameters in order to improve roughness of inclined surfaces on SLM manufactured parts within the same machine. This integrated SLM/LSR manufacturing method could provide a lean approach for improving inclined surface roughness, far beyond previously reported results (the average surface roughness values of less than1 µm), without requiring any additional facilities for surface modification process and eventually expand the capability of SLM process to fabricate components with wider applications in particular for 316L alloy.

2 Machine, Material and Method

2.1 Machine

For the purpose of this study, a commercially available Renishaw AM 250 selective laser melting (SLM) machine (Laser beam diameter: 70µm diameter at powder surface, Laser type: Ytterbium fiber laser, Laser wavelength: 1070 nm, Max laser power: 200 Watt) was utilized for

printing required samples. It should be noted that before conducting any experiment, AM 250 Machine parameters were calibrated by supplier team and based on its documented procedure.

2.2 Material

316L austenitic stainless steel powder (C < 0.03%, Mn < 2%, Si <1%, Cr 16~18%, Ni 10~14%, S < 0.03%, Mo 2-3%, O < 0.1%, N < 0.1%, P <0.045% , bal. Fe) was used for this study which was supplied by Renishaw plc. The particle size distribution of this powder was 45±15μm. Figure 1 displays the SEM of 316L austenitic stainless steel powder. As can be seen, the particles display round shape morphology with an appropriate size distribution.

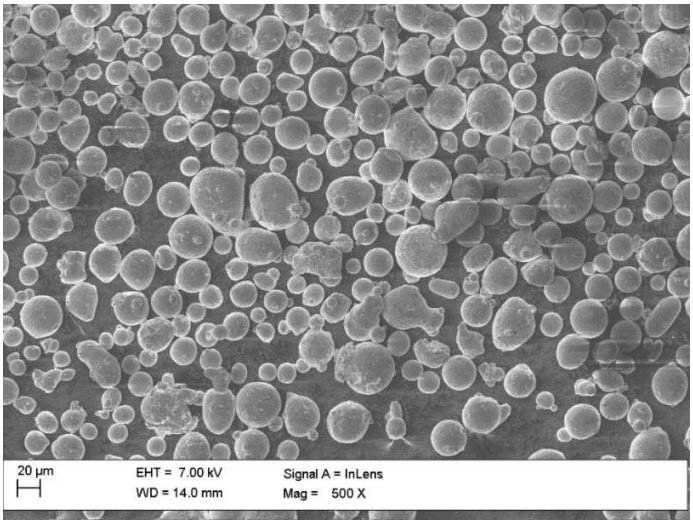

Fig. 1 SEM image of 316L austenitic stainless steel powder

2.3 Method

2.3.1 3D CAD-File Preparation

Optimizing vital laser surface re-melting process parameters (i.e. Laser power, Laser exposure time, Point distance, Shell layer thickness) on inclined surfaces to achieve minimum surface roughness was ultimate goal of this study. Therefore, for printing the required samples, predefined slider type CAD model with the 45° slope were created utilizing Magics® 19.02 software tools from Materialize Company. Then, several 4x4 test series (4 column and 4 rows) were printed at varying level of input parameters. Preliminary trial and error runs, machine technical specifications, and also a previously published work [8] were used for identifying the important input variables and the proper windows for those input parameters. Following objective of this study, for printing original samples, selective laser melting parameters were fixed at appropriate values (laser power: 160 Watt, laser exposure time: 110 μs, point distance: 50μm, layer thickness: 50μm, focal offset: 0 mm, scan strategy: meander). However, process parameters of laser surface re-melting step were varied according to section 2.5 of this paper. Figure 2 shows one of test series being printed for finding appropriate range of input parameters.

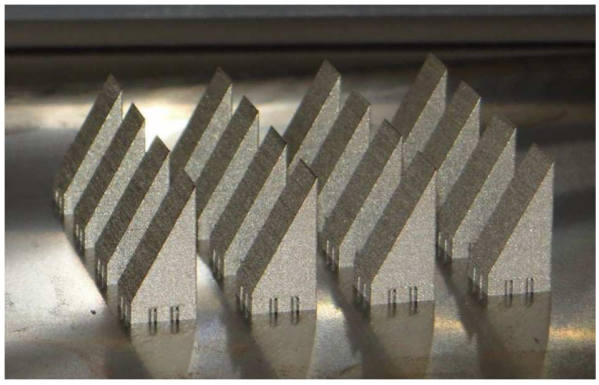

Fig. 2 4X4 printed test series

Then, twenty seven pieces of 45˚ inclined samples were printed to obtain the same range of original surface roughness (Ra=10.75 µm with a standard deviation of 1.85µm) by using CAD file of fig. 3-a. Additionally, in order to fully meet randomization assumption of statistical design of experiments, each sample series was printed separately [24]. After completion of printing of each sample, the substrate was moved upward (to the initial position) and the powder around the sample was removed completely. Then, predefined layer type CAD model with the 45˚ slope (Fig. 3-b) were also created using Magics® 19.02 software tools for implementing laser surface re-melting on inclined surface. Figure 3 shows CAD models for creating both base SLM part with support and laser surface re-melting surface shell in Magics® software.

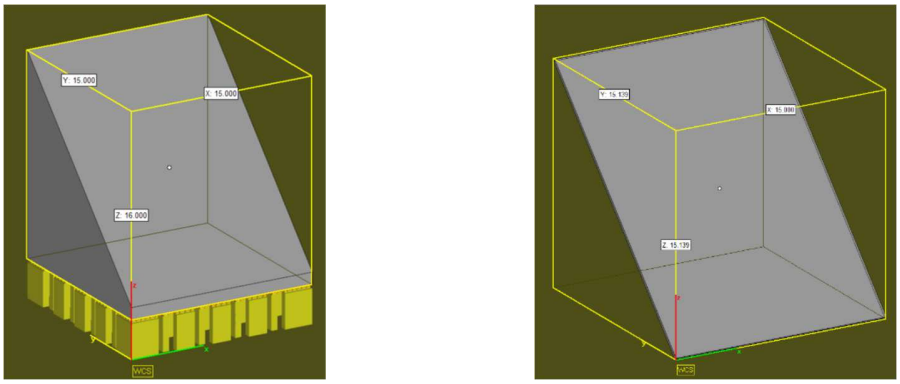

(a) (b)

Fig. 3 3D CAD models for (a) base SLM parts, (b) Laser surface re-melting shell

At this step, laser surface re-melting was conducted on the inclined surface of the printed sample. After completion of the re-melting process, sample was removed from the substrate for the evaluation of surface roughness. Figure 4 shows one of 27 samples after laser surface re-melting process and removal from the substrate. It should be noted that for all samples of this study, laser surface re-melting process was repeated three (3) times.

Fig. 4 Inclined SLM manufactured sample after applying SLR process

2.4 Surface Roughness Measurement

A Marsurf M300-C mobile roughness measuring instrument was used for measuring surface roughness (i.e. response) of inclined samples after mounting. Figure 5 shows this instrument set up for measuring roughness surface. For the purpose of accuracy, this instrument was calibrated frequently with pertinent surface roughness calibration block. The roughness tester measures both the arithmetic mean surface roughness (Ra) and the surface roughness depth (Rz). Since both measurements show the same trend, in this study the roughness of the samples are reported only by the arithmetic mean surface roughness (Ra). Since measuring surface roughness on inclined surface is very difficult, all 27 samples were mounted by using Buehler manual metallurgical sample mounting press. An example of roughness measurement on non-remelted (initial) surface and an example of roughness measurement on remelted (final) surface are presented in figs. 6 and 7 respectively.

Fig. 5 Roughness measuring instrument set up

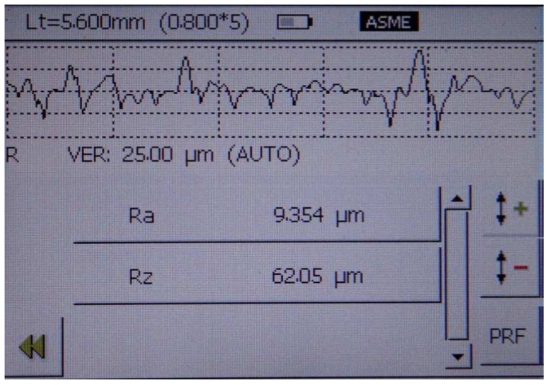

Fig. 6 A sample of roughness measurement on selective laser remelted surface (Before applying laser surface re-melting step)

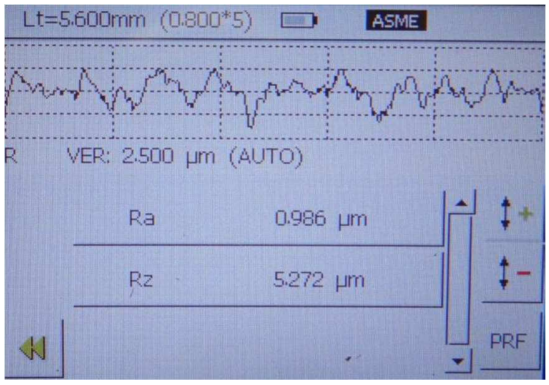

Fig. 7 A sample of roughness measurement on selective laser remelted surface (After applying laser surface re-melting step)

2.5 Response Surface Methodology Design

Based on literature review, in particular, for selective laser melting on stainless steel type 316L and also primary trials and errors experiments, four vital process parameters (Table 1) were selected for optimization of this laser surface re-melting process. The other process parameters were kept constant during this study. In this study, after setting ranges for the four independent variables, Box-Behnken design of experiment has been used for optimization purpose. Based on the Box-Behnken design, totally twenty seven (27) experiments were conducted with four independent variables.

Table 1 Parameters and ranges for Box-Behnken design of experiment

Dependent Variables	Coded and actual levels of dependent variables		
	-1	0	1
T: Shell Layer Thickness, µm	100	150	200
D: Point Distance, µm	30	50	70
E: Laser Exposure Time, µs	200	300	400
P: Laser Power, Watt	150	175	200

3 Results and Discussion

Table 2 illustrates 27 runs and results for Box–Behnken design of experiments. This table contains four input variables which are laser re-melting layer thickness, laser point distance, laser exposure time, and laser power in both coded and actual values. Based on this table, the minimum measured value for the response variable was observed in run 1 (Ra=0.76 μm) and the maximum measured response variable was observed in run 15 (Ra=6.83 μm) of this designed experiment. The succeeding sections aim to discuss table 2 in more detail.

Table 2 Input Variables in both coded and actual values

Run Order	Coded (Dimensionless) Input Variables				Actual Input Variables				Response Variable	
	T	D	E	P	T	D	E	P	Ym	Yp
1	0	0	+1	-1	150	50	400	150	0.76	0.91
2	-1	0	0	-1	100	50	300	150	3.43	3.68
3	-1	0	0	+1	100	50	300	200	2.45	2.22
4	0	0	-1	-1	150	50	200	150	6.00	5.97
5	0	0	0	0	150	50	300	175	1.85	1.85
6	0	+1	+1	0	150	70	400	175	2.27	1.98
7	0	0	+1	+1	150	50	400	200	1.45	1.46
8	-1	-1	0	0	100	30	300	175	3.84	3.73
9	+1	0	+1	0	200	50	400	175	2.20	2.29
10	0	0	-1	+1	150	50	200	200	4.68	4.70
11	0	+1	0	-1	150	70	300	150	3.22	3.02
12	0	+1	-1	0	150	70	200	175	4.83	4.60
13	0	-1	0	+1	150	30	300	200	3.60	3.72
14	0	-1	0	-1	150	30	300	150	4.60	4.28
15	0	-1	-1	0	150	30	200	175	6.83	7.19
16	+1	0	-1	0	200	50	200	175	6.21	6.24
17	0	+1	0	+1	150	70	300	200	2.62	2.85
18	-1	0	-1	0	100	50	200	175	5.65	5.47
19	0	0	0	0	150	50	300	175	1.65	1.85
20	0	0	0	0	150	50	300	175	2.06	1.85
21	+1	+1	0	0	200	70	300	175	3.54	3.63
22	-1	+1	0	0	100	70	300	175	2.92	3.29
23	+1	0	0	-1	200	50	300	150	3.24	3.55
24	+1	-1	0	0	200	30	300	175	5.71	5.32
25	0	-1	+1	0	150	30	400	175	1.20	1.51
26	-1	0	+1	0	100	50	400	175	1.25	1.13
27	+1	0	0	+1	200	50	300	200	4.45	4.28

T – Re-melting layer thickness (μm); D - Laser point distance (μm); E - Laser exposure time (μs); P - Laser power (Watt); Ym - Measured averaged roughness Ra (μm); Yp - Predicted roughness Ra (μm)

3.1 Main Effects of Independent Process Variables on Surface Roughness

Minitab® software and data from table 2 were used to calculate magnitudes of the main effects of the four vital input variables on surface roughness as dependent variable of this study (fig. 8).

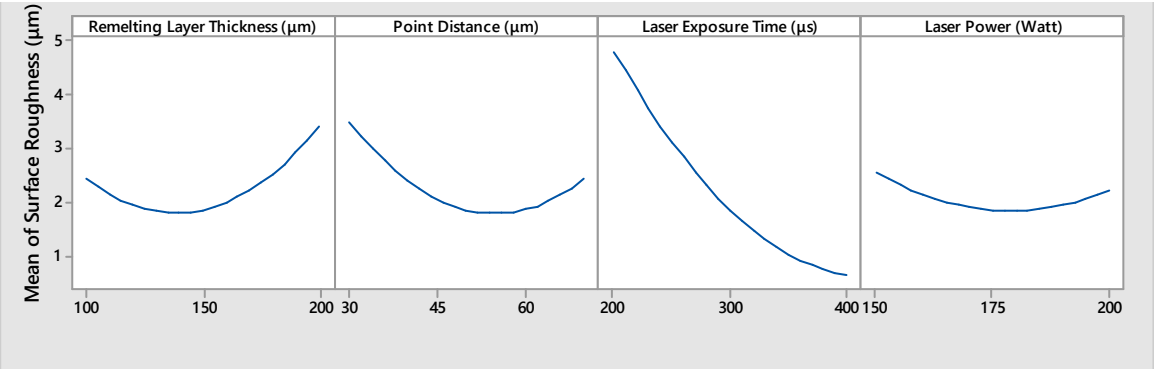

Fig. 8 Main effects plot for response (fitted means)

As fig. 8 indicates, at lower layer thickness, main effect of this factor is around 2.5 µm. Then, with the rise of layer thickness, main effect falls to about 1.6 µm, still with upturn of layer thickness further than 150 µm, this main effect again enhances substantially. Initial trial and error studies revealed that laser re-melting layer thickness less than 100 µm or beyond 500 µm deteriorates surface roughness and the former one also increases re-melting process time. At lower range of laser point distance, main effect of response variable on surface roughness is nearly 3 µm but with increase of this parameter, first this effect reasonably decreases and reaches a minimum value of about 2 µm and then again increase of point distance results in steady increase of remelted surface roughness. The main effects plots also show that laser exposure time has the greatest impact on surface roughness among four investigated parameters. At 200 µs of exposure, mean of response variable is nearby to 5 µm. With increase of this input parameter, the mean of response variable radically deceases. At the upper side of range for laser exposure time, this mean effect gradually hits a low point of 0.5 µm. Since main effects cannot explain the interaction among above mentioned four input variables, and their impacts on the response variable, the ANOVA procedure was utilized to study the possibility of cross-effects.

3.2 Analysis of Variance (ANOVA)

The common methodology for statistical modeling of process input variables is that at first step, fitness of a first-order regression equation is studied. If the first order regression model discloses notable lack of fit then the second order regression model is studied. ANOVA for the first order regression model shows sizable lack of fit (i.e. P-value>0.05 for Lack-of-Fit term, and R^2, R^2 adjusted, and R^2 predicted values respectively are 78.24%, 74.29%, and 70.65%). Consequently, at this stage it can be determined that range for input parameters of this study are not in distant area of response surface, and ranges of input parameters are appropriate for moving toward the valley of response surface. To put it another way, second order regression model should be a better fit for these set of experiments. At initial step of second order model fitting, full quadratic terms (i.e. linear, squares, and interactions) were included for fitting in analyzer module of Minitab® software [26]. In this work, in ANOVA procedure, p-value approach is being used for testing the hypothesis and will fail to reject H0 if statistic F0 is more than predefined (i. e. 0.05) alpha value. A first step ANOVA analysis (including all quadratic terms) for surface roughness illustrates that P-values of linear terms of T, D, and E, all square terms (T*T, D*D, E*E, P*P), and two way interaction terms of T*P, D*E, E*P statistically are significant and play a role in the response (surface roughness) regression equation in their specified processing ranges. However, two way interaction terms of T*E, D*P, and T*D

respectively have highest insignificant P-values (> 0.05) and should be taken away from ANOVA table step by step in order to approach to better fitted model.

Table 3 Analysis of Variance for surface roughness after removing insignificant terms

Source	DF	Adj SS	Adj MS	F-Value	P-Value
Model	11	73.6046	6.6913	57.65	0.000
Linear	4	58.9522	14.7381	126.97	0.000
T	1	2.8130	2.8130	24.23	0.000
D	1	3.3920	3.3920	29.22	0.000
E	1	52.4172	52.4172	451.59	0.000
P	1	0.3300	0.3300	2.84	0.112
Square	4	10.0770	2.5192	21.70	0.000
T*T	1	6.0161	6.0161	51.83	0.000
D*D	1	6.4338	6.4338	55.43	0.000
E*E	1	3.9982	3.9982	34.45	0.000
P*P	1	1.3986	1.3986	12.05	0.003
2-Way Interaction	3	4.5754	1.5251	13.14	0.000
T*P	1	1.1990	1.1990	10.33	0.006
D*E	1	2.3562	2.3562	20.30	0.000
E*P	1	1.0201	1.0201	8.79	0.010
Error	15	1.7411	0.1161		
Lack-of-Fit	13	1.6570	0.1275	3.03	0.275
Pure Error	2	0.0841	0.0420		
Total	26	75.3457			
Model Summary					
S	R-sq		R-sq(adj)		R-sq(pred)
0.340695	97.69%		95.99%		92.08%

As it is evident from table 3, all remaining terms of model have significant p-values apart from linear term laser point distance which has p-value of 0.112. Proposing an appropriate statistical model for forecasting cause and effect relationship among process input parameters and process outputs is among the key goals of statistical design of experiments analysis. By taking away all non-significant terms, the following revised regression model, in actual units, has been developed:

Yp (μm) = 86.3 - 0.1944 T - 0.4163 D - 0.1274 E - 0.4197 P + 0.000425 T*T + 0.002746 D*D + 0.000087 E*E + 0.000819 P*P + 0.000438 T*P + 0.000384 D*E + 0.000202 E*P

In the final ANOVA (table 3), p-value for lack-of-fit is 0.275 that is not statistically significant. In other words, above mentioned regression model does not expose any detectable lack-of-fit. In addition, R^2, R^2 adjusted, and R^2 predicted statistical parameters are presented in bottom of table 3. Typically approaching these statistical parameters to 100% are more appropriate. R^2 value of 97.69% is known as the determination coefficient. It implies that suggested regression equation can explain 97.69% of the variation in the response surface. R^2 adjusted value is 95.99%. In general, R^2 value increases with addition of a new term in the ANOVA table, but this new term does not always enhances the fitness of statistical regression model [27]. Hence, R^2 adjusted is a more suitable criterion to examine if adding a new term results in more accurate regression model. R^2 adjusted and R^2 values in ANOVA table are indicators for checking the current status of the regression model but R^2 predicted is more useful for checking level of fitness of the regression model for prospect observations of the under study

process. The R^2 predicted in the final ANOVA (table 3) which is very close to 100% (i.e. 92.08%) indicates fitness of proposed prediction model. Beside ANOVA, Box-Cox transformation concept was applied on collected data of table 2 in order to examine if there is any possibility for increasing equality of variance and normality over input variable ranges. By using Minitab software values of estimated λ and rounded λ are calculated as 0.96831 and 1, respectively. From the value of rounded λ it can be concluded that utilizing Box-Cox transformation has no remarkable effect on fitness of regression equation [28].

3.3 Validate Model Underlying Assumptions

For application of ANOVA analysis as a statistical technique, underlying assumptions need to be checked. First, the residual distribution of all independent and dependent parameters should follow a normal distribution. Assumption of homogeneity of variance is another issue that should be satisfied [24, 26, 28]. Figure 9 displays, the normal probability plot, the histogram, the residual versus fitted value, and the residual versus order for dependent variable of surface roughness. All these 4 plots imply that ANOVA underlying assumptions for dependent variable have been fulfilled.

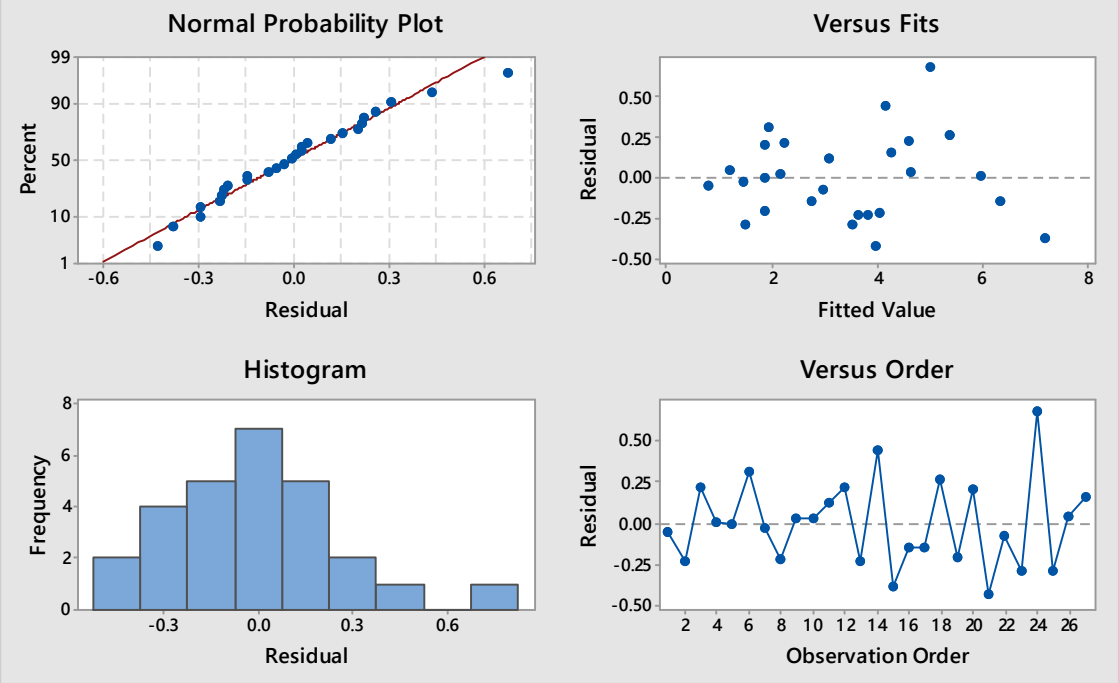

Fig. 9 Residual plots for response (Surface roughness)

3.4 Contour Plots of Response

Figures 10 represents six contour plot graphs for relationship between combinations of two of independent input variables (i.e. layer thickness, laser point distance, laser exposure time, and laser power) and surface roughness as dependent output variable. It can be seen, contour plot is an effective tool for visualizing the effects of process input variables on the process response

variable. The curvature of contours and elliptical graphs imply that process properly meets the second order model [26].

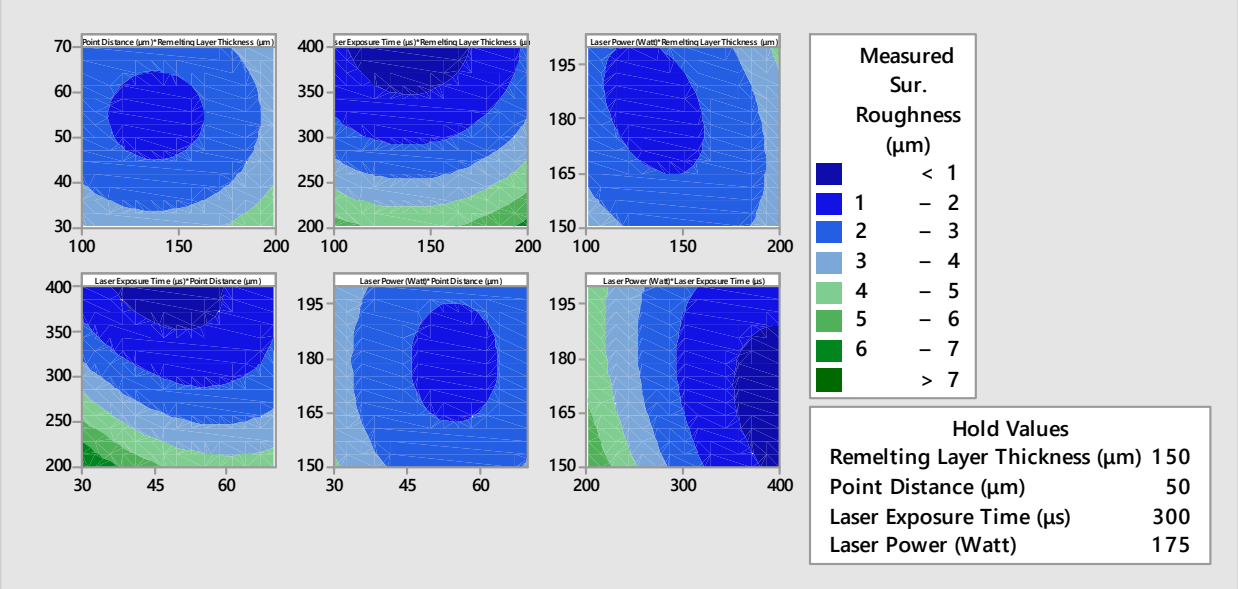

Fig. 10 Contour plots at average set of hold values

3.5 Response Optimization and Prediction Model Validation

One of the main goals of response surface methodology (RSM) as a statistical tool is to optimize input variables in order to obtain optimized response variable [26, 29-30]. By utilizing collected data from table 2 and response optimization module of Minitab software, optimized (minimum as the goal of this investigation) surface roughness (Yp=0.54) was attained at a set of 141.41µm of shell layer thickness, 47.77 µm of point distance, 400µs of laser exposure time, and 169.19 watt of laser power. It should be noted that each of these input values can be adjusted properly in order to evaluate the sensitivity of response roughness to subjective level of any input variables. For validation of proposed statistical prediction model, two samples were fabricated according to optimal set of input of process parameters. At these levels of laser surface re-melting process factors, expected surface roughness of 0.54 µm is expected. However, average of 0.68 µm surface roughness was measured on two validation samples. This implies that there is around 15% difference between measured and predicted responses.

3.6 SEM of Surface

Balling and satellites are reported as actual surface defects of SLM process [8, 11]. The unavoidable staircase or stair-step effect also plays a remarkable role in increasing the surface roughness which is due to layer by layer characteristic or dimensional gap between the 3D CAD model and the manufactured components of all AM processes [15, 31-32]. As it is clear from table 2, run 1 reveals the best surface roughness improvement among 27 runs of this study. Examining surface appearance and morphology of selective laser melting manufactured parts both before and after applying surface laser re-melting process is insightful for understanding the mechanisms and efficiency of re-melting process. Figure 11 shows SEM images of one SLM

printed samples both before and after laser surface re-melting at a magnification of about 100X and 400X for run 1 of this set of experiments. As these SEM images evidently disclose, laser surface re-melting practice on inclined surfaces has the capability to remarkably decrease unevenness of SLM manufactured inclined surfaces. Figure 11 images show at least two adjacent laser paths on top of laser surface re-melting area. In contrary to a previous publication [23], this result reveals that with optimized selection of process parameters, roughness in overlap area also could be improved significantly. This laser remelting result on 316L stainless is similar to results reported on Ti6AlV4 alloys with similar surface modification process [33]. Unlike the laser melting process where laser source interacts with metallic powder, in laser re-melting step, laser interacts with metallic surface which has remarkable peaks and valleys [34].

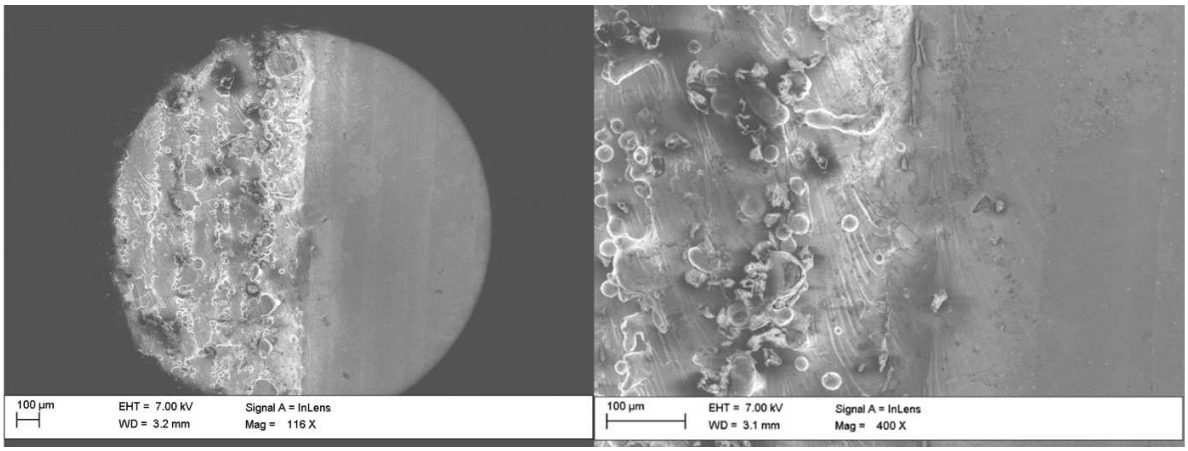

Fig. 11 SEM images of run 1 sample at two different magnifications (Left half of each image: Before re-melting process, Right half of each image: After remelting process)

Figure 12 further showed the microstructures of the re-melted surface. Re-melting hatch lines can be clearly observed in Fig. (a). Under 2000X magnification, Fig. 12b clearly shows the microstructures that consist of austenite grains and sigma phase grains, a well-known intermetallic phase, which forms in the Fe-Cr system [35]. While the sigma phase is an undesired phase possibly caused by laser heating, its effects to the integrity of the sample processed needs future investigation.

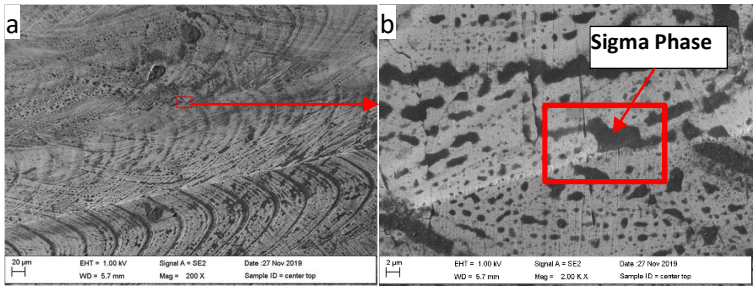

Fig. 12 SEM image of the sample showing the microstructures.

Figure 13 further demonstrates the grain structure in higher magnifications of the selected area in fig. 12b. Fig 13b shows cracks that were developed around the grain boundary , and in both b) and c), the cellular structure reported in related works is observed [36].

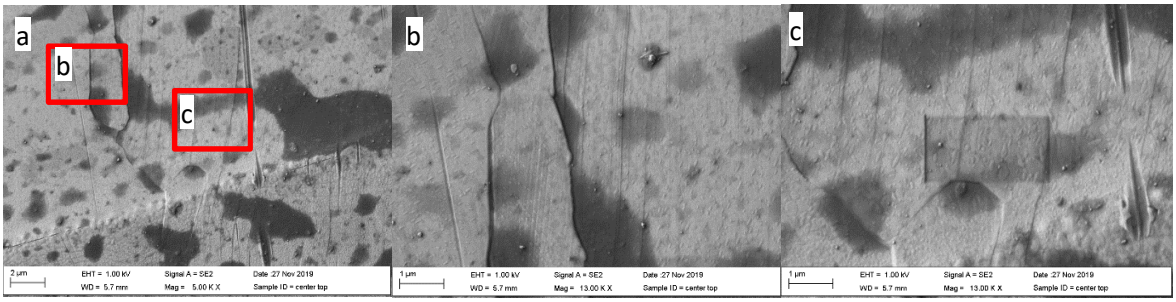

Fig. 13 Grain structure of the selected areas.

3.7 Importance of utilizing optimized process parameters

Figure 14 represents SLM printed and then surface remelted surfaces at extreme values of both laser power and laser exposure times. It is evident that utilizing very high levels of both laser exposure time and laser power (Fig. 14b) for surface remelting process lead to surface oxidation and very obvious uneven areas on remelted surface. On the other hand, utilizing very low levels of both laser exposure time and laser power (Fig. 14a) could not result in significance change in surface roughness. It should be noted that only implementation of optimized parameters of laser remelting on SLM printed parts can be effective and decrease surface roughness remarkably. Effect of laser remelting process parameters on microhardness and microstructure on the cross-section on the plan perpendicular to top surface are beyond the scope of this paper since reported in detail previously [37].

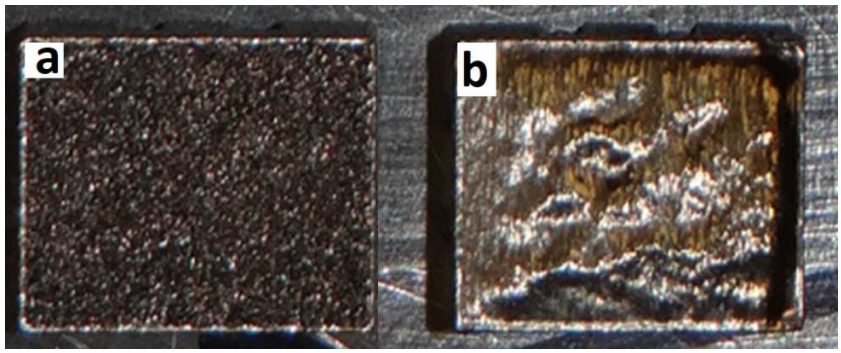

Fig.14 Nonoptimized surface remelting with extreme levels of remelting process parameters (a: Laser power (watt): 50, Laser exposure time (μs): 100 b: Laser power(watt):200, Laser exposure time (μs):1000)

4 Conclusions and Future Work

In this study, experiments were conducted by utilizing a Renishaw AM 250 selective laser melting (SLM) machine. The main conclusions are summarized as follows:

1) Findings from this investigation demonstrate that approaching to surface roughness of less than 1 μm in particular on 316L stainless steel inclined parts is feasible by an integrated selective laser melting and laser surface re-melting processes.

2) For re-melting of inclined 316L stainless steel surfaces, laser exposure time plays the most important role in improving surface roughness.

3) The results demonstrate that within the selected range, hatch distance has no effect on the roughness improvement on inclined surface re-melting but there is an optimal set point for layer thickness for the re-melting process. It should be noted that layer thickness of 50 μm and 100 μm widely are used for selective laser melting of 316L stainless steel parts, however, for consecutive laser re-melting a layer thickness of 200 μm could be applied. In other words, production rate of laser re-melting on inclined surfaces can be twice the selective laser melting process.

4) On contrary to previous studies, for integrated selective laser melting and laser surface re-melting process, it should be noted that optimized set of process parameters for selective laser melting will not necessarily be optimized for laser re-melting process as well. In other words, process parameters of these two processes should be optimized separately.

5) Optimized set of process parameters for selective laser melting or laser surface re-melting on horizontal surface will not necessarily be optimized for the same process on all inclined surfaces. In other words, process parameters of inclined, horizontal, and vertical surfaces should be optimized separately.

6) With increasing slope angle, laser surface re-melting process covers less surface area therefore this method would be faster at lower angels (i.e. $< 60^{o}$).

7) For our purpose, this study focused on re-melting of 45^{o} inclined surfaces. Optimization of re-melting process parameters for other (lower and higher) inclined angles, which were beyond resources and scope of this study, could also be examined and optimized.

8) For the purpose of this study, the substrate was fixed and just moved in Z direction in the SLM system. However for re-melting of geometrically complex parts, giving more degrees of freedom and rotation to the either substrate or laser power source could increase desirability of this hybrid approach. Integrating DOE and machine learning techniques may also increase efficiency of this hybrid approach.

9) SEM of the remelted samples showed small cracks and sigma phase. While sigma phase was reported in other works related to SLM, its impact to desire surface quality needs further study in the future.

Acknowledgement: Studies are supported by the DoD/ARO grant W911NF-14-1-0083, Renishaw Cooperative Industry Funding, and the Dr. Bose Family donation.

References

[1] Ngo, Tuan D., Alireza Kashani, Gabriele Imbalzano, Kate TQ Nguyen, and David Hui. "Additive manufacturing (3D printing): A review of materials, methods, applications and challenges." *Composites Part B: Engineering* (2018).

[2] Frazier, William E. "Metal additive manufacturing: a review." *Journal of Materials Engineering and Performance* 23, no. 6 (2014): 1917-1928.

[3] Lee, Jian-Yuan, Jia An, and Chee Kai Chua. "Fundamentals and applications of 3D printing for novel materials." *Applied Materials Today* 7 (2017): 120-133.

[4] Bikas, H., Panagiotis Stavropoulos, and George Chryssolouris. "Additive manufacturing methods and modelling approaches: a critical review." *The International Journal of Advanced Manufacturing Technology* 83, no. 1-4 (2016): 389-405.

[5] Brytan, Z. "Comparison of Vacuum Sintered and Selective Laser Melted Steel AISI 316L." *Archives of Metallurgy and Materials* 62, no. 4 (2017): 2125-2131.

[6] AlMangour, Bandar, Dariusz Grzesiak, and Jenn-Ming Yang. "In-situ formation of novel TiC-particle-reinforced 316L stainless steel bulk-form composites by selective laser melting." *Journal of Alloys and Compounds* 706 (2017): 409-418.

[7] Alsalla, Hamza Hassn, Christopher Smith, and Liang Hao. "Effect of build orientation on the surface quality, microstructure and mechanical properties of selective laser melting 316L stainless steel." *Rapid Prototyping Journal* 24, no. 1 (2018): 9-17.

[8] Wang, Di, Yang Liu, Yongqiang Yang, and Dongming Xiao. "Theoretical and experimental study on surface roughness of 316L stainless steel metal parts obtained through selective laser melting." *Rapid Prototyping Journal* 22, no. 4 (2016): 706-716.

[9] Yakout, Mostafa, M. A. Elbestawi, and Stephen C. Veldhuis. "On the characterization of stainless steel 316L parts produced by selective laser melting." *The International Journal of Advanced Manufacturing Technology* 95, no. 5-8 (2018): 1953-1974.

[10] Khorasani, AmirMahyar, Ian Gibson, Moshe Goldberg, and Guy Littlefair. "Production of Ti-6Al-4V acetabular shell using selective laser melting: possible limitations in fabrication." *Rapid Prototyping Journal* 23, no. 1 (2017): 110-121.

[11] Covarrubias, Ernesto E., and Mohsen Eshraghi. "Effect of Build Angle on Surface Properties of Nickel Superalloys Processed by Selective Laser Melting." *JOM* 70, no. 3 (2018): 336-342.

[12] Brown, D., C. Li, Z. Y. Liu, X. Y. Fang, and Y. B. Guo. "Surface integrity of Inconel 718 by hybrid selective laser melting and milling." *Virtual and Physical Prototyping* 13, no. 1 (2018): 26-31.

[13] Casalino, G., S. L. Campanelli, N. Contuzzi, and A. D. Ludovico. "Experimental investigation and statistical optimisation of the selective laser melting process of a maraging steel." *Optics & Laser Technology* 65 (2015): 151-158.

[14] Baicheng, Zhang, Lee Xiaohua, Bai Jiaming, Guo Junfeng, Wang Pan, Sun Chen-nan, Nai Muiling, Qi Guojun, and Wei Jun. "Study of selective laser melting (SLM) Inconel 718 part surface improvement by electrochemical polishing." *Materials & Design* 116 (2017): 531-537.

[15] Boschetto, Alberto, Luana Bottini, and Francesco Veniali. "Roughness modeling of AlSi10Mg parts fabricated by selective laser melting." *Journal of Materials Processing Technology* 241 (2017): 154-163.

[16] Boschetto, A., L. Bottini, and F. Veniali. "Surface roughness and radiusing of Ti6Al4V selective laser melting-manufactured parts conditioned by barrel finishing." *The International Journal of Advanced Manufacturing Technology* 94, no. 5-8 (2018): 2773-2790.

[17] Pyka, Grzegorz, Andrzej Burakowski, Greet Kerckhofs, Maarten Moesen, Simon Van Bael, Jan Schrooten, and Martine Wevers. "Surface modification of Ti6Al4V open porous structures produced by additive manufacturing." *Advanced Engineering Materials* 14, no. 6 (2012): 363-370.

[18] Baicheng, Zhang, Lee Xiaohua, Bai Jiaming, Guo Junfeng, Wang Pan, Sun Chen-nan, Nai Muiling, Qi Guojun, and Wei Jun. "Study of selective laser melting (SLM) Inconel 718 part surface improvement by electrochemical polishing." *Materials & Design* 116 (2017): 531-537.

[19] Ciubotariu, Costel-Relu, Doina Frunzăverde, Gabriela Mărginean, Viorel-Aurel Șerban, and Aurel-Valentin Bîrdeanu. "Optimization of the laser re-melting process for HVOF-sprayed Stellite 6 wear resistant coatings." *Optics & Laser Technology* 77 (2016): 98-103.

[20] Alfieri, Vittorio, Paolo Argenio, Fabrizia Caiazzo, and Vincenzo Sergi. "Reduction of surface roughness by means of laser processing over additive manufacturing metal parts." *Materials*10, no. 1 (2016): 30.

[21] Alrbaey, K., D. Wimpenny, Riccardo Tosi, Warren Manning, and Adam Moroz. "On optimization of surface roughness of selective laser melted stainless steel parts: a statistical study." *Journal of Materials Engineering and Performance* 23, no. 6 (2014): 2139-2148.

[22] Kruth, Jean-Pierre, Evren Yasa, and Jan Deckers. "Roughness improvement in selective laser melting." In *Proceedings of the 3rd international conference on polymers and moulds innovations*, pp. 170-183. 2008.

[23] Yasa, Evren, and Jean-Pierre Kruth. "Application of laser re-melting on selective laser melting parts." *Advances in Production engineering and Management* 6, no. 4 (2011): 259-270.

[24] Box, George EP, William Gordon Hunter, and J. Stuart Hunter. "Statistics for experimenters." (1978).

[25] Delgado, Jordi, Joaquim Ciurana, and Ciro A. Rodríguez. "Influence of process parameters on part quality and mechanical properties for DMLS and SLM with iron-based materials." *The International Journal of Advanced Manufacturing Technology* 60, no. 5-8 (2012): 601-610.

[26] Montgomery, Douglas C. *Design and analysis of experiments*. John wiley & sons, 2017.

[27] Wu, Zhenhua, Jianzhi Li, Douglas Timmer, Karen Lozano, and Subhash Bose. "Study of processing variables on the electrical resistivity of conductive adhesives." *International Journal of Adhesion and Adhesives* 29, no. 5 (2009): 488-494.

[28] Osborne, Jason W. "Improving your data transformations: Applying the Box-Cox transformation." *Practical Assessment, Research & Evaluation* 15, no. 12 (2010): 2.

[29] Akia, Mandana, Hamidreza Arandiyan, Karen Lozano, and Seyed Mahdi Alavi. "Optimizing the dehydrogenation catalyst of higher normal paraffins supported on a nanocrystalline gamma alumina." *Catalysis Science & Technology* 6, no. 15 (2016): 5982-5991.

[30] Akia, Mandana, Dulce Capitanachi, Misael Martinez, Carlos Hernandez, Hector de Santiago, Yuanbing Mao, and Karen Lozano. "Development and optimization of alumina fine fibers utilizing a centrifugal spinning process." *Microporous and Mesoporous Materials* 262 (2018): 175-181.

[31] Tolochko, Nikolay K., Sergei E. Mozzharov, Igor A. Yadroitsev, Tahar Laoui, Ludo Froyen, Victor I. Titov, and Michail B. Ignatiev. "Balling processes during selective laser treatment of powders." *Rapid Prototyping Journal* 10, no. 2 (2004): 78-87.

[32] Yadroitsev, I., Pavel Krakhmalev, I. Yadroitsava, Sten Johansson, and I. Smurov. "Energy input effect on morphology and microstructure of selective laser melting single track from metallic powder." *Journal of Materials Processing Technology* 213, no. 4 (2013): 606-613.

[33] Vaithilingam, J., Goodridge, R. D., Hague, R. J., Christie, S. D., Edmondson, S. "The effect of laser remelting on the surface chemistry of Ti6al4V components fabricated by selective laser melting." Journal of Materials Processing Technology 232 (2016): 1-8.

[34] Bhaduri, D., Penchev, P., Batal, A., Dimov, S., Soo, S. L., Sten, S., ... & Dong, H. (2017). Laser polishing of 3D printed mesoscale components. Applied Surface Science, 405, 29-46.

[35] Kou, S. Welding Metallurgy, 2nd ed.; John Wiley & Sons, Inc.: Hoboken, NJ, USA, 822 (2003)

[36] Yasa, Evren, Jan Deckers, and Jean-Pierre Kruth. "The investigation of the influence of laser re-melting on density, surface quality and microstructure of selective laser melting parts." Rapid Prototyping Journal 17.5 (2011): 312-327.

[37] Kožuh S., Goji´M., Kosec L., Kovove Materialy - Metallic Materials 47 (2009): 253–262